Management of metabolic and reproductive disturbances in letrozole induced polycystic ovarian syndrome by Asparagus racemosus roots

Angshita Ghosh
Vidyasagar University
Sananda Sil
Vidyasagar University
Tarun Kumar Kar
Vidyasagar University
Ananya Barman
Vidyasagar University
Sandip Chattopadhyay
sandipdoc@yahoo.com
Vidyasagar University

Research Article

Keywords: PCOS, Asparagus racemosus, Hyperandrogenism, Inflammation, Apoptosis, Androgen receptor

Posted Date: July 11th, 2024

DOI: https://doi.org/10.21203/rs.3.rs-4472411/v1

Additional Declarations: No competing interests reported.

Abstract

Background: Polycystic Ovary Syndrome (PCOS) has emerged as a widespread endocrine health challenge for women in the childbearing phase by imposing an adverse influence on fertility. Unfortunately, the existing treatment-strategies are inadequate and largely focused on symptom-based relief. Therefore, the demand for safer herbal alternatives is more pressing than ever.Asparagus racemosus Willd. has a longstanding history as a traditional herb for addressing diverse hormonal and fertility complications. The present study explored the in-depth mechanism by which A. racemosus ethanolic extract (ARE) ameliorates PCOS in female adult rats.

Methods: ARE at different doses (100, 150, 250 mg/kg-bw) were concurrently supplemented in the letrozole-induced PCOS group (1 mg/kg-bw) for a continuous period of 21 days. LC/ESI-MS was employed for determination of active phytotherapeutics within the ARE. Biochemical assay, ELISA, native PAGE expression, Real-time PCR, immunostaining and histological study were implemented for the experimental analysis.

Results: ARE regularized the disrupted estrous pattern, improved metabolic status and balanced endocrine activity by reducing excess androgen production. ARE restored intraovarian antioxidant enzyme expression and markedly reduced the mRNA expression of inflammatory (NFkB/TNFα) and proapoptotic markers (Bax/P53) along with elevated expression of anti-apoptotic factor (BCL2). The downregulation of androgen receptor (AR) in ovarian tissue accompanied by a decreased in the angiogenic factor VEGF-B were also observed. ARE improved gonadal weights and histomorphology by limiting the formation of cystic follicles and promoting folliculogenesis. The presence of essential secondary metabolites, specifically steroidal sapogenin, isoflavones and polyphenols, is primarily responsible for these advantageous effects.

Conclusion: The observed findings suggested that A. racemosus could be a highly effective safer alternative therapeutic intervention for managing the complexities of PCOS.

Background

Polycystic ovarian syndrome (PCOS) is a prevailing endocrinopathy in women of reproductive age, characterized by hyperandrogenism, irregular menses and cystic morphology, which ultimately lead to ovarian oligo/anovulatory dysfunction, infertility and metabolic disturbances [1, 2]. Elevated androgen levels disrupt the HPG axis, leading to a persistent increase in the GnRH pulse and excessive secretion of LH compared to FSH [3]. Hyperandrogenaemia additionally contributes to steroidogenic abnormalities and premature luteinization and hinders folliculogenesis with the progression of follicular atresia [4]. Generally, androgens exert their action through the androgen receptor (AR) across various tissues and the altered AR signaling pathway has been acknowledged as a potential determinant of ovulatory ailments in PCOS patients [5]. Moreover PCOS patients also experience metabolic comorbidities including obesity, insulin resistance (IR) and dyslipidaemia which are associated with an elevated risk of glucose intolerance [2]. Androgen-driven preadipocyte differentiation enhances lipolysis by increasing

FFA release, which further induces lipotoxicity with endoplasmic reticulum (ER)-mediated stress in the follicular microenvironment [6]. Excess androgen combined with IR triggers systemic inflammation and elevates intraovarian oxidative damage, ultimately compromising follicular maturation and oocyte quality [7]. Prolonged and persistent inflammation in the ovarian microenvironment triggers granulosa cell (GC) pyroptosis through activating ER-stress, which impacts ovarian function, conception, and implantation processes in women diagnosed with PCOS [8]. Moreover, aberrant vascularization accompanied by decreased ovulation rates and increased granulosa cell apoptosis may also contribute to the development of multiple ovarian cysts in PCOS individuals [9].

The exact etiological mechanism of PCOS is still a matter of controversy and lacks clear elucidation, contributing to the complexity of executing medical diagnoses and interventions for this syndrome. Modern therapeutic interventions, including oral contraceptive pills and insulin sensitizers, primarily offer short-term symptom-based relief with the frequent occurrence of substantial adverse effects. These circumstances necessitate further research to explore potential alternative herbal therapeutic approaches for PCOS management and mitigate the side effects that adversely affect quality of life. The incorporation of traditional and ayurvedic herbs into the regular diet has emerged as a novel trend in the treatment of various health ailments [10].

Asparagus racemosus Willd., commonly popular as Shatavari or Shatamuli (Asparagaceae family), is a well-documented Ayurvedic medicinal plant with fleshy tuberous roots. This herbs is typically found in tropical and subtropical regions of India and the Himalayas [11]. In Ayurveda, Shatavari is renowned as a versatile feminine tonic that contributes to the nourishment of reproductive organs and the enhancement of fertility [12]. The primary Ayurvedic medicinal scriptures Ashtang Hridyam and Charak Samhita highlighted the usage of *A. racemosus* in formulations designed to address female reproductive disorders [13, 14]. The presence of principal bioactive metabolites including steroidal saponins (shatavarins), sapogenins, asparosides, isoflavones, flavonoids, fructo-oligosaccharides, glycosides, sterols, fatty acids and minerals, in *A. racemosus* roots results in diverse therapeutic and pharmacological actions [15]. These roots exhibit phytoestrogenic properties, contributing to the regulation of hormonal balance and the stimulation of folliculogenesis and ovulation [16, 17]. Additionally, previous studies have shown that antidiabetic, hypolipidaemic, antioxidant, adaptogenic, antihepatotoxic, antineoplastic, immunoadjuvant, anti-inflammatory, galactogogue and neuroprotective effects without causing side effects [15]. Despite considerable research on the remedial efficacy of *A. racemosus*, traditional knowledge must be connected with contemporary evidence-based pharmacology for treating PCOS. Hence, the present investigation evaluated the impact of *A. racemosus* on endocrine, metabolic and reproductive profiles in LET-induced PCOS management to address the existing knowledge gap in this area.

Materials and Methods

Reagents

Letrozole tablets were obtained from Sun Pharmaceutical Ltd, Bengaluru, India. All the consumables were obtained from Hi Media (India), and Merck (India).

Selection and verification of the plant specimens

Asparagus racemosus roots were purchased from local market (Vyas Pharmaceuticals; A GMP Certified Unit; Mfg. Lic. No. 25D/11/93; Batch no: 00181) in Midnapore, West Bengal. The root sample of *A. racemosus* was authenticated by Dr. Dulal Kumar De (Botany Department, Midnapore College, West Bengal, India) for certification.

Phytochemical investigations

Preparation of A. racemosus hydroethanolic extract (ARE)

The conventional maceration process was used to carry out the extraction [18]. The powdered roots of the *A. racemosus* were uniformly soaked in solvent (70% ethanol and 30% distilled water) at a 1:10 ratio for approximately 72 hours with occasional shaking. Subsequently, the liquid herbal extract was filtered using Whatman filter paper and collected filtrate was concentrated by a rotary vacuum evaporator. The resultant semisolid extracts were air-dried and further subjected to qualitative phytochemical investigation.

Liquid chromatography- electrospray ionization-mass spectrometry (LC-ESI-MS) profiling

The presence of possible bioactive ingredients was identified by LC-MS analysis via a mass spectrometer microTOF-Q connected to a UPLC Water Acquity system following the method of Wojakowska *et al.*, 2013 [19]. Combinations of two different solvents, A (H_2O 99.5%; formic acid v/v 0.5%) and B (acetonitrile 99.5%; formic acid v/v 0.5%), were used to accomplish chromatographic separation on EC-C18 coloumns with a 2:1 effluent ratio at 0.6 ml/min flow rate. The extract solution (5 ml) was introduced into the LC/MS apparatus following the specific gradient elution process. The MS was performed in both negative and positive ESI ion modes using ideal ionization and fragmentation settings with a mass range from 100–1000 m/z for maximum metabolome coverage.

Experimental Design

Ethical consideration

The Committee of Animal Ethics at Vidyasagar University was granted approval for this present project (ethical clearance number VU/IAEC/.CPCSEA/19/7/2022 dt.22.11.2022), adhering to the recommendations defined by the CPCSEA (Committee for the Purpose of Control and Supervision of Experiments on Animals), India.

Animal housing

Female virgin Wistar strain albino rats (8–12 weeks of age and 120 ± 20 g body weight) with regular estrous cycle were housed in a standardized environment (12-hour light–dark cycle, 25 ± 2°C temperature and 55–65% humidity) for the purpose of acclimatization prior to the experiment. Throughout the experimental period, the rats were provided with standard pellet meal and water ad libitum.

Study design

A total of thirty-six animals were arbitrarily distributed into the following six groups, each comprising of six rats (n = 6).

1. **Control Group (CON)**: Orally administered 0.5% CMC (Carboxymethyl cellulose) as a vehicle.
2. **PCOS or LET group**: PCOS induction in the animals was accomplished by administering Letrozole (LET) orally at a dosage of 1 mg/kg body weight (BW), dissolved in CMC (0.5%) [20].
3. **ARE 100 group**: Oral-administration of LET (1mg/kg) + ARE supplementation at 100 mg/kg-bw dose [21].
4. **ARE 150 group**: Received LET (1mg/kg) + ARE supplementation at 150 mg/kg-bw dose via oral route [21].
5. **ARE 250 group**: Oral-administration of LET (1mg/kg) + ARE supplementation at 250 mg/kg-bw dose [22].
6. **MET group**: Orally received LET (1mg/kg) + Metformin (MET) at 250 mg/kg-bw dose [23].

The total duration of experiment was for 21 consecutive days. On day 22, the rats were anesthetized via ketamine-HCl intramuscular injection (24 mg/kg-bw dose) for the procurement of blood and organs [24]. Subsequently, the animals were euthanized using barbiturate.

Measurement of physical parameters

Body mass and organosomatic indices

The alteration in body mass of each animal was regularly monitored from the commencement of the experiment up to the point of sacrifice. Variations in body weight across the groups frequently make it difficult to compare the organ weights of treated and untreated animals. Therefore, the organosomatic indices were computed based on the following ratios:

Organosomatic indices (gm %) = [organ weight (gm)/ body weight (gm) * 100] [25].

Estrous cycle

The various phases of the estrous cycle are associated with hormonal fluctuations, which are also indicative of reproductive health. The estrous stages were evaluated by observing vaginal cytology. Vaginal cells were gently collected and examined microscopically after Leishman staining. Based on the presence and ratios of nucleated epithelial cells, cornified nonnucleated cells and leukocytes, the estrous phases were detected.

Biochemical estimation

Metabolic profile

Serum was separated from blood samples to assess metabolic parameters by centrifuging for 10 minutes at 2500 rpm. Commercially available kits acquired from ENZOPAK were used to evaluate fasting glucose, triglycerides (TG), and total cholesterol (TC) levels in accordance with the manufacturer recommendations. The triglyceride-glucose (TyG) index (indicator of insulin resistance), was further calculated by the following equation:

TyG index = Ln [TG (mg/dl) × FPG (mg/dl)/2] [26].

Gonadotropins and sex steroids

The plasma concentrations of LH (luteinizing hormone; ELK Biotechnology; mIU/ml; Cat: ELK2367), FSH (follicular stimulating hormone; ELK Biotechnology mIU/ml; Cat: ELK1315) testosterone (ng/ml; ELK Biotechnology; Cat: ELK8314) and progesterone (ng/ml; Cat: ELK8385) were quantified by sandwich and competitive ELISA (enzyme-linked immuno sorbent assay) following the protocols mentioned in the manufacturer's guidelines.

Inflammatory cytokines and adipokines

The proinflammatory markers IL-6 (pg/mol; ABclonal; cat no. RK00020), TNF-α (ng/mol; ABclonal; cat no. RK00029), NFκB (ng/mol; ELK Biotechnology; cat no. ELK5691) and the adipokine leptin (pg/ml; ABclonal; cat no. RK03790) were quantified by sandwich and competitive ELISA, based on the given procedure in the respective kit catalog.

Steroidogenic enzymes, growth factors and cell cycle regulators

The concentrations of 3βHSD (fine test; cat no. ER0665), the angiogenic growth factor VEGF-B (ng/ml; fine test; cat no.ER0085) and the cell cycle regulator CCND-1 (ng/ml; fine test; cat no. ER0328) in ovarian tissue were estimated using ELISA following the Wuhan Fine Test Kit protocol.

Electrozymographic native-page expression analysis

Homogenization of the ovarian tissue (50 mg) was performed using chilled phosphate buffered saline (PBS; pH 7.4) following centrifugation (15 min at 12000 rpm) after which the supernatant was collected. Following the methodology described by Weydert and Cullen (2010) [27], the electrophoresis was conducted on the 12% native page for the expression of superoxide dismutase (SOD), while catalase and glutathione peroxidase (GPx) were expressed on the 8% native page. A gel documentation apparatus (Bio-Rad) was used to visualize the patterns of the achromatic bands and the band densities were analyzed using ImageJ software.

Reverse Transcription and Real-Time PCR

Ovarian mRNA expression of the NF-kB, TNF-α, p53, Bax and Bcl2 genes was assessed through RT-PCR (Applied Biosystems, 7900HT, USA). Total ovarian RNA (50 mg) was purified using TRIzol RNA isolation reagent (GCC Biotech, India). cDNA (complementary DNA) synthesis was performed by reverse transcription process using a Himedia, cDNA synthesis kit. Subsequently, amplification of cDNA was carried out via RT-PCR using SYBR Mastermix (GCC Biotech) and specific primers, based on the fluorescence-based detection technique. The relative mRNA expression was computed by analyzing the cycle threshold (Ct value) of the amplification curve following the $2^{-\triangle\triangle Ct}$ method [28]. The data are expressed as the mean value of the fold change relative to the control ± SE, where GAPDH is the reference gene.

Histomorphometric and immunohistochemical analysis

The ovaries and uterus were subjected to a systematic procedure involving fixation in neutral formalin (10%) for 48 hours, following paraffin embedding. Subsequently, the specimens were serially sectioned longitudinally at 5 µm thickness using a microtome and stained with hematoxylin and eosin (H & E). The stained tissue sections were examined under a light microscopic system (Olympus CX21i trinocular) for histomorphological evaluation.

Immunohistochemistry was performed to evaluate the expression of androgen receptor (NR3C4) in ovarian tissue sections. Ovarian tissue sections were immersed in citrate buffer (0.1 M; pH 6.0) for antigen retrieval. Following the blocking with BSA (bovine serum albumin, 3%), the sections were incubated with primary antibodies for overnight at 4°C. After the washing steps, the secondary antibody (polyperoxidase IgG conjugate) was simultaneously applied to the tissue section for 2 hours. Following the development of a brownish color using DAB (3, 3’-diaminobenzidine) solution, the slides were further counterstained with hematoxylin. A light microscope (Olympus CX21i trinocular) was used to obtain immunostaining images to visualize morphological alterations at receptor level. Semiquantification analysis of the images was carried out using Fiji ImageJ2 software based on the percentage of the thresholding area of the DAB stain [29].

Statistical analysis

ANOVA followed by the Post Hoc Tukey’s t-test was used to calculate the statistical significance of differences among distinct groups. The data are expressed as mean ± SE; n = 6 in each group.

Results

Phytochemical profiling of A. racemosus

LC-ESI-MS profiling of *A. racemosus* revealed the presence of 21 bioactive metabolites such as sarsasapogenin (416.51 m/z); schidigerasaponin D5 (740.29 m/z); shatavarin IV (887.08 m/z); shatavarin VII (883.44 m/z); shatavarin VI (885.13 m/z); shatavarin IX (901.79 m/z); shatavarin X (926 m/z); cinnamic acid(148.29 m/z); β-sitosterol (415.91 m/z); apigenin (269.82 m/z); isoquercetin (464.05 m/z); 8-methoxy-5,6,4'-trihydroxy-isoflavone-7-o-β-D-glucopyranoside (479.02 m/z); quercetin (302.23

m/z); stigmasterol (412.27 m/z); kaempferol (285.25 m/z); γ-linoleinic acid (278.30 m/z); ferulic acid (194.79 m/z); racemosol (340.48 m/z); immunoside (870.02 m/z); gallic acid (170.88 m/z) and genistein (270.24 m/z) (Fig. 1). Tentative identification of the bioactive components in the present study was performed based on the MS data analysis and comparison with previously reported information. The typical LC-MS-based chromatogram peaks of ARE are representative of metabolome coverage in the mass range 100–1000 m/z (Fig. 1). The molecular formula, chemical class, MS data and retention time (RT) of each component are listed in Table 1.

Table 1
Category wise representation of possible bioactive phytoconstituents present in the ethanolic extract of *Asparagus racemosus* analysed by LC-ESI/MS.

	RT (Min)	Phytochemicals Name	Chemical Formula	Mass (m/z)	Type of metabolites
1	1.306	Sarsasapogenin	C27H44O3	416.51	Steroidal sapogenin
2.	1.306	Schidigerasaponin D5	C39H64O13	740.29	Steroidal saponin
3.	1.306	Shatavarin IV	C45H74O17	886.14	Steroidal saponin
4.	1.306	Shatavarin IX	C45H74O18	901.79	Steroidal saponin
5.	14.74	Cinnamic acid	C9H8O2	148.69	Phenolic acid
6.	15.62	Apigenin	C15H10O5	269.82	Flavonoid
7.	15.62	Genistein	C15H10O5	270.76	Isoflavones
8.	15.62	Beta sitosterol	C29H50O	415.91	Phytosterol
9.	16.30	Shatavarin VII	C47H76O19	884.25	Steroidal saponin
10.	16.30	Shatavarin V	C45H74O17	885.13	Steroidal saponin
11.	16.30	Immunoside	C45H74O16	870.02	Glycoside
12.	17.75	Shatavarin X	C47H76O18	926.00	Steroidal saponin
13.	18.42	Kaempferol	C15H10O6	194.79	Flavonoid
14.	18.42	Racemosol	C21H24O4	340.48	Alkalloids
15.	18.42	Isoquercetin	C21H20O12	464.05	Isoflavone
16.	18.42	8-Methoxy-5,6,4'-trihydroxy-isoflavone-7-o-β-D-glucopyranoside	C22H22O12	479.02	Isoflavone
17.	19.25	Quercetin	C15H10O7	300.56	Isoflavone

18.	19.25	Stigmasterol	C29H48O	412.27	Phytosterol
19.	23.98	Gallic acid	C7H6O5	170.88	Polyphenol
20.	23.98	Gamma linoleinic acid	C18H30O2	278.30	Fatty acid
21.	23.98	Stigmasterol-β-d-glucoside	C35H58O6	574.46	Phytosterol

Physiological changes

The LET-induced PCOS group exhibited a significant ($P < 0.001$) increase in body weight (43.25%) compared to the vehicle-treated control group (14.62%) (Table 2). This increase in weight indicated successful PCOS induction by LET. ARE supplementation at a 250 mg/kg-bw dose in LET-fed rats substantially ($P < 0.001$) decreased body weight gain (20.76%) compared with that in the PCOS group (Table 2), highlighting the therapeutic potential of ARE for promoting weight loss. Similarly, compared with PCOS, MET administration also significantly ($P < 0.001$) lowered weight gain by 20.09%.

Table 2

Effect of *Asparagus racemosus* on bodyweight and organosomatic indices (%).Data represent as Mean ± SEM (n = 6), estimated by ANOVA following the post hoc Tukey's test *P < 0.05, **P < 0.01, ***P < 0.001 in respect to control; #P < 0.05, ##P < 0.01, ###P < 0.001 in respect to LET group.

Groups	Initial body weight (IBW)	Final body weight (FBW)	Organo-somatic indices (%)	
			Ovarian index (OI)	Uterine index (UI)
CON	110.50 ± 2.04	126.66 ± 3.89	0.042 ± 0.003	0.238 ± 0.015
LET	112.50 ± 2.74	161.16 ± 3.80***	0.060 ± 0.003**	0.094 ± 0.009***
ARE 100	111.50 ± 2.26	155.00 ± 3.26	0.050 ± 0.005	0.121 ± 0.009
ARE 150	109.50 ± 1.17	144.16 ± 3.30$^{\#}$	0.048 ± 0.003	0.134 ± 0.010
ARE 250	111.16 ± 2.19	134.33 ± 3.30$^{\#\#\#}$	0.046 ± 0.002$^{\#}$	0.149 ± 0.015$^{\#}$
MET	108.66 ± 2.24	130.50 ± 1.72$^{\#\#\#}$	0.051 ± 0.004	0.128 ± 0.011

LET-induced PCOS rats also demonstrated a significant ($P < 0.05$) increase in ovarian weight and decrease in uterine weight ($P < 0.001$) than those in the control group. This outcome suggested disruptions in ovarian function coupled with a reduction in the size of the uterine horn. Moreover, LET-fed rats administered with ARE (250 mg/kg-bw), exhibited a notable ($P < 0.001$) increase in uterine weight and a significant decrease in ovarian weight ($P < 0.05$) (Table 2). No statistically significant difference

was detected in utero-ovarian weight ($P > 0.05$) subsequent to treatment with 100mg/kg ARE, 150mg/kg ARE and 250 mg/kg MET.

Changes in estrous cyclicity

The vehicle-treated control group displayed a normal 4–5 day estrous duration consisting of four successive phases: proestrus, oestrus, metestrus and dioestrus. Following LET treatment for 21 days, estrus cyclicity was arrested in the dioestrus phase, as confirmed by the presence of leukocytes in the vaginal fluid. This complete disruption of the estrous pattern also confirmed successful PCOS development in rats. Administration of ARE (250 mg/kg-bw) in combination with LET resulted in greater proportions of proestrus (epithelial nucleated cells) and estrus (cornified nonnucleated cells) phases along with a shorter duration of the disestrus phase (Fig. 2), indicating a more robust estrous pattern than in the PCOS group. Moreover, the MET group displayed almost similar patterns as did the ARE-supplemented group.

Metabolic changes

LET treatment resulted in a notable increase in the serum FBG ($P < 0.001$), TC ($P < 0.05$), TG ($P < 0.001$) and TyG index ($P < 0.001$) compared to those of the control (Fig. 3). These findings emphasize the development of hyperglycemia, insulin resistance and dyslipidemia in the PCOS group. No substantial improvement was noted following 100 mg/kg ARE therapy whereas 150 mg/kg ARE markedly reduced FBG, TG and the TyG index. Moreover, compared with the PCOS treatment, the 250 mg/kg ARE dose significantly ameliorated the metabolic profile in LET-fed rats (Fig. 3), indicating the anti-diabetic and hypolipidemic effects. This improvement was evident through the reduction in levels of FBG ($P < 0.01$), TG ($P < 0.05$) and TC ($P < 0.001$) levels coupled with an improved TyG index ($P < 0.001$). Similarly, significant improvements in the metabolic profile were also noted in the MET group.

Hormonal changes

A significant increase in the serum LH ($P < 0.001$) and testosterone ($P < 0.001$) levels, coupled with a decrease in the FSH ($P < 0.01$) and progesterone ($P < 0.001$) levels, was evident after LET treatment (Fig. 4), suggesting that hyperandrogenism mediated hormonal imbalance in PCOS group. The administration of ARE 250 mg/kg therapy in combination with LET effectively rectified this hormonal imbalance by reducing LH ($P < 0.05$) and testosterone ($P < 0.05$) levels and enhancing FSH ($P < 0.05$) and progesterone ($P < 0.05$) levels (Fig. 4). The ARE 150 group displayed a significantly improved LH/FSH ratio whereas no such difference was detected in the ARE 100 group. These findings suggested the hormone modulatory action of ARE against PCOS. However, compared with LET-treatment, MET significantly ($P < 0.05$) decreased testosterone levels.

Changes in 3βHSD and CCND1 levels

Steroidogenic disruption in the LET-induced PCOS group was confirmed by the increase in 3βHSD concentration ($P < 0.001$) compared to that in the control (Fig. 4). Additionally, the significant increase in

CCND1 (P < 0.01) indicated an altered cell cycle transition from G1 to S phase. In contrast, the 250 mg/kg ARE treatment significantly decreased both 3βHSD (P < 0.01) and CCND1 (P < 0.01) levels, indicating potential steroidogenic and cell cycle regulatory effects (Figs. 4 and 5). ARE supplementation at a dose of 150 mg/kg-bw also significantly decreased the concentration of 3βHSD. No significant difference was detected following MET and 100 mg/kg ARE treatment.

Changes in plasma leptin

The LET-treated group exhibited a marked increase in the plasma leptin level (P < 0.001) relative to that in the normal control group (Fig. 5), implying a positive association with central adiposity in PCOS rats. However, compared with the PCOS treatment, the 150 and 250 mg/kg revealed antiadipogenic effects on PCOS, as indicated by a noteworthy reduction in the plasma leptin concentration (p < 0.001) (Fig. 5). The ARE 100 group also exhibited less significant improvement in leptin levels (P < 0.01) than the other two doses. Like in the ARE 250 group, leptin levels were also lower in the MET-treated group (P < 0.001).

Changes in cytokines

The substantial increase in NFκB (P < 0.001), TNF-α (P < 0.01) and IL-6 (P < 0.001) levels, as well as in the VEGF-B concentration (P < 0.001) suggested systemic inflammation with abnormal ovarian vascularity in the PCOS group. Conversely, compared with 100 and 150 mg/kg doses of ARE, 250 mg/kg ARE therapy combined with LET more effectively relieved these condition by lowering NF-κB (P < 0.001), TNF-α (P < 0.05), IL-6 (P < 0.05) and VEGF-B (P < 0.001) levels (Fig. 5). Moreover, significant decreases in IL-6 (P < 0.05) and NFκB (P < 0.001) were detected with MET-administration.

Changes in antioxidant status

The LET-induced PCOS group decreased the protein band density of SOD (P < 0.001), catalase (P < 0.001) and GPx (P < 0.001), emphasizing the imbalance in intraovarian redox status. Supplementation with 250 mg/kg ARE in combination with LET significantly increased the protein expression of SOD (P < 0.001), catalase (P < 0.001) and GPx (P < 0.001) compared with that in the PCOS group by decreasing intraovarian oxidative stress (Fig. 6). Similarly, the MET group demonstrated a comparatively greater band density of anti-oxidative enzymes like the ARE supplemented group.

Changes in mRNA expression

The LET-group presented significantly greater fold change in the expression of the P53 (3.87-fold; P < 0.001), BAX (8.74-fold; P < 0.001), NFKB (7.15-fold; P < 0.01) and TNF-α (7.34-fold; P < 0.01) genes and these changes were accompanied by a decrease in the expression of the BCL2 gene (0.17-fold; P < 0.01). The upregulation of proinflammatory and apoptotic expression combined with the downregulation of antiapoptotic gene expression (Fig. 7) in PCOS group caused inflammation-mediated systemic activation of ovarian apoptosis. However, comparative with LET, 250 mg/kg ARE therapy substantially reduced the fold change in the expression of P53 (0.90-fold; P < 0.01), BAX (3.36-fold; P < 0.05), NFKB (3.12-fold; P <

0.01) and TNF-α (2.80-fold; $P < 0.05$) along with a greater fold change in the expression of BCL2 (0.72-fold; $P > 0.05$) (Fig. 7).These observed expression patterns demonstrated the antiinflammatory and antiapoptotic effects of ARE. MET-treatment also improved the fold change similar to the ARE 250 group.

Changes in ovarian histomorphology

The ovarian sections of the LET-group exhibited altered histomorphology, characterized by multiple immature cystic follicles with a destructive granulosa cell layer. Severe impairment of primordial and primary follicles occurred with increased follicular atresia and luteal regression in the PCOS group, indicating that hyperandrogenism mediated anovulation (Fig. 8A; Table 3). The ovarian histoarchitecture was restored comparatively better in ARE 250 group than in the ARE 100 and 150 group, as indicated by a notable reduction in the number of cystic follicles and the presence of mature follicles with prominent granulosa layers. Moreover, the presence of a corpus luteum and the regeneration of previously damaged primordial and primary follicles were also detected following ARE therapy (Fig. 8; Table 3) because they improve the folliculogenesis process. However, MET administration also resulted in fewer cysts with the reappearance of corpus luteum and other healthy follicles.

Table 3
Effect of *Asparagus racemosus* on ovarian follicular count, granulosa layer thickness, uterine endometrium width and secretory glands. Data represent as Mean ± SEM (n = 6), estimated by ANOVA following the post hoc Tukey's test *P < 0.05, **P < 0.01, ***P < 0.001 in respect to control; #P < 0.05, ##P < 0.01, ###P < 0.001 in respect to LET group.

	CON	LET	ARE 100	ARE 150	ARE 250	MET
Primary follicles	24.83 ± 2.00	10.66 ± 0.88***	13.83 ± 1.66	15.00 ± 2.20	18.66 ± 1.72#	20.50 ± 2.14##
Secondary follicles	13.16 ± 1.01	3.16 ± 0.47***	6.83 ± 1.13	7.33 ± 1.14	9.16 ± 0.94##	8.83 ± 1.13##
Tertiary follicles	8.50 ± 0.76	1.50 ± 0.42***	3.33 ± 0.49	4.16 ± 1.07	4.33 ± 0.49#	2.83 ± 0.30
Corpus luteum	9.83 ± 0.47	2.83 ± 0.40***	3.83 ± 0.60	5.66 ± 0.76#	6.33 ± 0.49##	5.66 ± 0.49#
Cystic follicles	0.17 ± 0.16	9.50 ± 0.84***	8.16 ± 1.01	6.00 ± 0.85#	4.16 ± 0.30###	5.83 ± 0.60##
Atretic follicles	5.16 ± 0.40	13.16 ± 0.47***	11.00 ± 1.41	8.00 ± 0.96##	5.50 ± 0.56###	5.66 ± 0.71###
Granulosa cell thickness	49.51 ± 4.21	18.60 ± 1.92***	23.86 ± 2.20	31.95 ± 3.34#	35.84 ± 3.68#	33.85 ± 1.52#
Endometrium width	154.89 ± 5.83	91.37 ± 4.90***	105.08 ± 4.27	113.57 ± 4.59#	120.75 ± 5.54##	109.74 ± 5.31
Endometrial glands	17.83 ± 0.94	7.16 ± 1.19***	6.60 ± 0.84	8.50 ± 1.23	12.16 ± 0.60##	8.83 ± 0.79

Changes in uterine morphology

Uterine photomicrographs of the LET-group revealed a thin uterus characterized by lessening of endometrial secretory glands and a reduction in endometrial width compared to those of the control group (Fig. 8B; Table 3). However, compared with the PCOS group, the administration of ARE (250 mg/kg) combined with LET resulted in a comparative improvement in the number of uterine glands with endometrial walls. Supplementation with 150 mg/kg ARE also resulted in a noteworthy increase in endometrial length whereas no such change was demonstrated in the 100 mg/kg ARE group. The MET group also exhibited increased endometrial width and glands but these changes were not significant.

Changes in ovarian AR or NR3C4

The expression and localization of the NR3C4 protein were significantly evident in the ovarian tissue sections of the LET-induced PCOS group, in which the immunoreactivity was greater in the theca and

degenerative granulosa layers of cystic follicles and interstitial cells. This observation indicated that hyperandrogenism-induced impaired thecal AR or NR3C4 signalling, which further worsened ovarian dysfunction. In contrast, the 250 mg/kg ARE treatment group exhibited comparatively weaker AR expression and immunoreactivity in follicular granulosa and thecal cells, suggesting that ARE regulates the NR3C4 receptor (Fig. 9A). The semiquantative investigation of the immunostained images revealed a 1.95-fold ($P < 0.001$) increase in the AR or NR3C4 receptor in LET-treated rats relative to those in the control group. Moreover, compared with LET-treatment, 250 mg/kg ARE administration led to a 1.56-fold ($P < 0.001$) reduction in AR expression (Fig. 9B). The MET group also displayed similar findings as did the ARE-supplemented group.

Discussion

The successful establishment of a PCOS rat model with various metabolic and reproductive phenotypes similar to those of human PCOS has been well documented with the use of Letrozole [20]. In line with the findings of previous investigations, our results also revealed an abnormal estrous cycle, hormonal imbalance, metabolic alterations, inflammation and ovulatory dysfunction following LET treatment for 21 consecutive days [30, 31]. The present investigation suggested the positive impact of ARE on alleviating the diverse symptoms associated with LET-induced PCOS. The most bioactive secondary metabolites found in ARE previously demonstrated a wide range of therapeutic potential in maintaining metabolic, neuroendocrine and reproductive homeostasis.

Hyperandrogenism and steroidogenic abnormalities in PCOS negatively affect the HPG axis and gonadotropin release [3]. Similarly, the LET-induced PCOS group exhibited hyperandrogenism, as indicated by increased serum testosterone levels (Fig. 4). This excess androgen accumulation eventually disrupted the function of the HPG axis, leading to overactivation of LH and suppression of FSH [32]. Additionally, increased concentrations of ovarian 3βHSD in response to excess LH secretion resulted in steroidogenic disruption and hormonal imbalance in PCOS individuals [31]. Alterations in circulating sex steroids contributed to an abnormal estrous cycle with a prolonged diestrus phase in LET-induced PCOS (Fig. 2).

The neuroendocrine actions of ARE decreased LH hypersecretion and maintained the proper gonadotrophic (LH:FSH) ratio in the PCOS group by modulating the HPG-axis and GnRH pulsatile secretion. The most prominent neutraceuticle of ARE, sarsasapogenin (416.51 m/z) previously displayed HPG-axis regulatory properties via the Kiss1/GPR54 system, which subsequently balanced gonadotropes [33]. Moreover, ARE administration alleviated excess androgen production by limiting the concentration of the ovarian steroidogenic enzyme 3βHSD, which further improved hormone fluctuations and typical estrous patterns. A previous investigation suggested that apigenin inhibits 3βHSD through interference with the steroidogenic pathway, resulting in indirect suppression of testosterone production [34]. Moreover, isoflavones and quercetin both exhibit testosterone lowering activity and estrous cycle regularity in letrozole-induced PCOS animals [35, 36]. Additionally, both the phytotherapeutic genistein and the isoflavones of ARE have been shown to antagonize AR expression by regulating the

transcriptional activation and nuclear translocation of AR [37]. Thus ARE supplementation mitigated hyperandrogenism-mediated excessive AR signalling in ovarian tissue (Fig. 9), improving the GC layer and ovulatory functions.

Previous evidence has indicated that excess androgen in women with PCOS often disturbs systemic metabolism by enhancing fat deposition and insulin resistance [2]. The LET-induced PCOS group exhibited a spike in fasting glucose and triglyceride levels, which contributed to a high TyG index (Fig. 3). The TyG index is a reliable indicator for assessing insulin resistance in the present study [38]. A hyperglycemic state increases free testosterone in the bloodstream by decreasing SHBG production while insulin resistance triggers theca cells to produce more androgens [39]. Insulin resistance is strongly associated with hyperleptinemia, which plays a crucial role in the development of obesity by affecting peripheral tissues [40].The LET-treated PCOS group exhibited greater leptin levels and increased body weight, suggesting an association with increasing adiposity in the present study (Fig. 5; Table 2).

Metabolic disruptions associated with PCOS were effectively reversed following ARE therapy, which improved hyperandrogenism mediated insulin resistance, leading to enhanced glucose and lipid metabolism. The antihyperglycemic effect of ARE significantly reduced blood glucose levels and increased insulin secretion, as confirmed by the decrease in the TyG index (Fig. 3). Quercetin regulates glucose by activating AMPK/insulin-independent pathways, enhancing GLUT-4 receptors on the cell membrane to facilitate glucose uptake [41]. The suppression of the key enzymes involved in gluconeogenesis and the protection of β-cells by quercetin [42], contributed to the antidiabetic effects of ARE. ARE administration also decreased triglyceride and cholesterol levels (Fig. 3) by regulating androgen-driven lipid homeostasis. The hypolipidemic efficacy of ARE was likely due to the presence of β-sitosterol, which was previously shown to lower blood cholesterol levels by impeding its absorption in the intestines [43]. γ -Linolenic acid in ARE was previously shown to decrease leptin levels by upregulating PPAR-γ signalling [44]. Thus ARE supplementation reduced PCOS-induced central adiposity with hyperleptinemia by promoting lipolysis and decreasing lipogenesis (Fig. 5).

Although free radicals are essential for regulating ovarian physiological processes, excessive ROS production can increase the risk of ovarian dysfunction by altering intraovarian redox [45]. Previously, an LET-induced PCOS model showed the involvement of oxidative stress and an inflammatory state in the formation of cystic follicles [31]. The reduced expression of ovarian antioxidative enzymes (SOD, CAT and GPx) in the present study suggested a greater rate of oxidative stress in the LET-treated group (Fig. 6). This oxidative stress further stimulates the activation of proinflammatory mediators that may lead to hyperandrogenism and IR [46]. Additionally, hyperinsulinemia promotes granulosa cell (GC) apoptosis, which ultimately results in follicular atresia and ovulatory disorders [8]. Our results also demonstrated increased expression of proinflammatory (NFκB, TNFα and IL-6) and proapoptotic (P53 and Bax) mediators but reduced expression of antiapoptotic (BCL2) markers following LET administration (Fig. 7).

The potent antioxidative action of ARE enhances the expression of endogenous antioxidant enzymes and neutralizes the excessive intraovarian ROS production triggered by metabolic alterations in the PCOS group. Moreover, apigenin significantly decreases total oxidative stress (TOS) levels and increases total antioxidant capacity (TAC) in the ovarian tissues of individuals with PCOS [47]. Moreover, quercetin was also proven to enhance SOD, CAT and GPx activities by inhibiting NADPH oxidase, safeguarding cells from oxidative damage-induced lipid peroxidation [36]. Moreover, the ARE also subsequently inhibited the OS-linked redox-sensitive activation of ovarian inflammatory and apoptotic signalling in PCOS rats which might result in improved cellular homeostasis. The presence of sarsasapogenin was previously reported to suppress LPS-induced acute tissue inflammation by halting IKK/NF-kB/JNK mediated inflammatory signalling [48]. Sarsasapogenin decreases site-specific phosphorylation of IKK and JNK while increasing IκB-α protein levels, collectively contributing to the inactivation of NFκB transcription [48, 49]. However, ferulic acid also impeded NFkB activation by reducing proinflammatory mediators (TNF-α and IL-6) and hindering the STAT1/PIAS1 downstream signalling pathway [50]. Therefore, ARE suppressed NFkB-TNF-α-IL-6 mediated ovarian tissue inflammation, which further improved the follicular microenvironment and minimized ovarian ailments in PCOS rats. Moreover, ARE attenuated OS-mediated ovarian cellular apoptosis by suppressing proapoptotic BAX and P53 expression and enhancing antiapoptotic BCL2 expression (Fig. 7). Thus ARE could play a critical role in normalizing the follicular maturation process and improving oocyte quality. In the ARE, gallic acid regulates the expression of the apoptotic markers BAX and BCL2, modulating PI3K/AKT signalling [51]. In addition, ARE also controlled the overactivation of CCND1 and prevented abnormal cell cycle phase transition. The presence of cinnamic acid in ARE limits excessive cellular proliferation by inhibiting Cyclin D1 [52].

PCOS individuals often experience abnormal angiogenesis, characterized by increased stromal vascularisation and increased levels of proangiogenic markers [9]. Deregulation of ovarian vascularization in LET-induced PCOS was strongly modified following ARE supplementation by preventing the overproduction of the proangiogenic factor VEGF-B (Fig. 5). Activation of the VEGF gene occurs when androgens bind to AR binding sites located within its promoter region [53]. The phenolic compound gallic acid has been shown to demonstrate an antiangiogenic effect on ovarian cells through the modulation of PTEN/AKT/HIF-1α/ VEGF signalling [54]. ARE-mediated restoration of appropriate angiogenic siganalling during the ovarian cycle may further facilitate ovulation and corpus luteum formation by regulating folliculogenesis.

Consistent with earlier investigations, our results revealed the presence of multiple cystic follicles with degenerative granulosa layers, increased follicular atresia and reduced secretory glands with endometrial walls in the histomorphology of the ovaries and uterus of the PCOS group [30, 31]. The hyposecretion of FSH impairs the follicular maturation process and development of the corpus luteum, leading to decreased secretion of progesterone in PCOS group [55]. The rejuvenating action of ARE restored gonadal weight and morphology in PCOS rats through the regulation of hormonal and inflammatory signalling. This further enhanced the proliferation of healthy follicles with proportionate thecal vascularization and reduced cyst formation and follicular atresia. The restoration of the follicular ovulatory process following ARE therapy was confirmed by the appearance of secondary and tertiary

follicles with thickened granulosa layers and developing oocytes in the PCOS group (Fig. 8A). Moreover, ARE maintained luteinization regularity and upregulated the growth of the corpus luteum which further increased progesterone levels (Figs. 4 and 8A). The corpus luteum is acknowledged for its vital role in progesterone secretion, a key factor in governing reproductive cycles and preparing the uterus for potential conception [56]. The phytoprogestin-like property of kaempferol thickens the uterine lining by regulating the expression of progesterone-associated genes [57]. In addition, β-sitosterol also regulates endometrial receptivity in individuals with PCOS via harmonized reproductive hormonal levels [58]. Thus, ARE renovated uterine morphology by maintaining uterine weight, endometrial width and the number of secretory glands in PCOS group (Fig. 8B).

Taken together, the present investigation provides the fresh evidence that compared with the standard drug metformin, ARE at a dosage of 250 mg/kg bw is better able to reverse endrocrinal dysregulation in PCOS. In addition, the oxidative stress, angiogenic and metabolic regulatory properties of ARE strongly support the use of *A. racemosus* as an alternative supplementary therapeutic approach for addressing PCOS and associated fertility issues. Nevertheless, additional exploration is necessary to assess the prolonged usage of this herb and its efficacy compared with the other PCOS drugs.

Conclusion

Overall, we elucidated the possible descriptive anti-PCOS mechanism of ARE through the restoration of hyperandrogenism-mediated PCO, metabolic abnormalities, inflammatory/apoptotic alterations and distorted reproductive histomorphology. The observed effectiveness was attributed to the specific combined activity of the potent phytotherapeutics present in this herb. However, whether the complex intervention of these phytocomponents of *A. racemosus* is involved in synergistic or antagonistic interactions for the execution of the therapeutic potential of ARE has not yet been determined. Moreover, there is a lack of research regarding the pharmacological action of the ARE-specific steroidal saponin shatavarins. Identification and characterization of the proper therapeutic function of these components are essential for future drug development.

Abbreviations

3βHSD
3-beta-hydroxysteroid dehydrogenase
IL-6
Interleukin-6
NFκB
Nuclear factor kappa-light-chain-enhancer of activated B cells
TNFα
Tumor necrosis factor alpha
BCL2
B-cell lymphoma 2

BAX
Bcl2-associated X-protein
P53
Tumor Protein p53
VEGF-B
Vascular endothelial growth factor B
CCND1
Cyclin D1
NR3C4
Nuclear receptor subfamily 3, group C, member 4
PAGE
Polyacrylamide Gel Electrophoresis
GAPDH
Glyceraldehyde-3-phosphate dehydrogenase.

Declarations

Ethics approval and consent to participate:

The Committee of Animal-Ethics in Vidyasagar University was granted the approval for this present project (ethical clearance number VU/IAEC/.CPCSEA/19/7/2022 dt.22.11.2022), adhering to the recommendations defined by the CPCSEA (Committee for the Purpose of Control and Supervision of Experiments on Animals), India.

Consent for publication:

Not applicable.

Competing interest:

All authors declare that there are no competing interest.

Funding:

This study is partially funded by the research fellowship Savitribai Jyotirao Phule Single Girl Child Fellowship (Grant no. 202223-UGCES-22-GE-WES-F-SJSGC-2817).

Author Contribution

Angshita Ghosh contributed to the conceptualization, methodology, immunostaining, real-time PCR and manuscript writing. Animal treatment, biochemical assay and gel electrophoresis were performed by

Sananda Sil and Tarun Kumar kar. ELISA and statistical data analysis were performed by Ananya Barman. Experimental protocol design and manuscript editing were performed by Sandip Chattopadhyay. All authors reviewed the manuscript and approved for the submission.

Acknowledgement:

Not applicable.

Data availability:

Data will be made available on request.

References

1. Escobar-Morreale HF. Polycystic ovary syndrome: definition, aetiology, diagnosis and treatment. Nat Rev Endocrinol. 2018;14(5):270–84.
2. Sanchez-Garrido MA, Tena-Sempere M. Metabolic dysfunction in polycystic ovary syndrome: pathogenic role of androgen excess and potential therapeutic strategies. Mol Metab. 2020;35:100937.
3. Liao B, Qiao J, Pang Y. Central Regulation of PCOS: Abnormal Neuronal-Reproductive-Metabolic Circuits in PCOS Pathophysiology. Front Endocrinol (Lausanne). 2021;12:667422.
4. Palomba S, Daolio J, La Sala GB. Oocyte Competence in Women with Polycystic Ovary Syndrome. Trends Endocrinol Metab. 2017;28(3):186–98.
5. Gao XY, Liu Y, Lv Y, Huang T, Lu G, Liu HB, Zhao SG. Role of Androgen Receptor for Reconsidering the true polycystic ovarian Morphology in pcos. Sci. Rep., Botella-Carretero M, Benguria JI, Villuendas A, Zaballos G, San A, Millán JL, Escobar-Morreale HF, Peral B. Differential gene expression profile in omental adipose tissue in women with polycystic ovary syndrome. J Clin. Endocrinol. Metab. 2007; 92(1): 328 – 37.
6. Orisaka M, Mizutani T, Miyazaki Y, Shirafuji A, Tamamura C, Fujita M, Tsuyoshi H, Yoshida Y. Chronic low- grade inflammation and ovarian dysfunction in women with polycystic ovarian syndrome, endometriosis, and aging. Front Endocrinol (Lausanne). 2023;14:1324429.
7. Repaci A, Gambineri A, Pasquali R. The role of low-grade inflammation in the polycystic ovary syndrome. Mol Cell Endocrinol. 2011;335(1):30–41.
8. Di Pietro M, Pascuali N, Parborell F, Abramovich D. Ovarian angiogenesis in polycystic ovary syndrome. Reproduction. 2018;155(5):R199–209.
9. Lakshmi JN, Babu AN, Kiran SSM, Nori LP, Hassan N, Ashames A, Bhandare RR, Shaik AB. Herbs as a Source for the Treatment of Polycystic Ovarian Syndrome: A Systematic Review. BioTech (Basel). 2023;12(1):4.

10. Alok S, Jain SK, Verma A, Kumar M, Mahor A, Sabharwal M. Plant profile, phytochemistry and pharmacology of *Asparagus racemosus* (Shatavari): A review. Asian Pac J Trop Dis. 2013;3(3):242–51.
11. Sharma K, Bhatnagar M. Asparagus racemosus (Shatavari): A versatile female tonic. Int J Pharm Biol Arch. 2011;2(3):855–63.
12. Garde GK, Vagbhat S. Marathia translation of vagbhat's astangahridya, Uttarstana: Aryabhushana Mudranalaya. 1970; 1970: 40–48.
13. Sharma RK, Dash B. Charaka samhita-text with english translation and critical exposition based on Chakrapani Datta's Ayurveda dipika. India: Chowkhamba Varanasi; 2003.
14. Majumdar S, Gupta S, Prajapati SK, Krishnamurthy S. Neuro-nutraceutical potential of Asparagus racemosus: A review. Neurochem. Int. 2021; 145: 105013.
15. Pandey AK, Gupta A, Tiwari M, Prasad S, Pandey AN, Yadav PK, Sharma A, Sahu K, Asrafuzzaman S, Vengayil DT, Shrivastav TG, Chaube SK. Impact of stress on female reproductive health disorders: Possible beneficial effects of shatavari (Asparagus racemosus). Biomed. Pharmacother. 2018;103:46–9.
16. Lalert L, Kruevaisayawan H, Amatyakul P, Ingkaninan K, Khongsombat O. Neuroprotective effect of Asparagus racemosus root extract via the enhancement of brain-derived neurotrophic factor and estrogen receptor in ovariectomized rats. J Ethnopharmacol. 2018;225:336–41.
17. Rasul MG. Conventional extraction methods use in medicinal plants, their advantages and disadvantages. Int J Basic Sci Appl Comput. 2018;2:10–4.
18. Wojakowska A, Perkowski J, Góral T, Stobiecki M. Structural characterization of flavonoid glycosides from leaves of wheat (Triticum aestivum L.) using LC/MS/MS profiling of the target compounds. J Mass Spectrom. 2013;48(3):329–39.
19. Kafali H, Iriadam M, Ozardali I, Demir N. Letrozole-induced polycystic ovaries in the rat: a new model for cystic ovarian disease. Arch Med Res. 2004;35(2):103–8.
20. Mandal SC, Nandy A, Pal M, Saha BP. Evaluation of antibacterial activity of Asparagus racemosus willd. root. Phytother Res. 2000;14(2):118–9.
21. Vishwakarma P, Chatterjee M, Sharma M, Saini M, Goel R, Saxena KK. Evaluation of Cardioprotective activity of Asparagus racemosus against Doxorubicin induced cardiotoxicity in albino rats, an experimental study. Int J Basic Clin Pharmacol. 2019;8(7):1693.
22. Rani R, Sharma AK, Chitme HR. Therapeutic Effect of Tinospora cordifolia (Willd) Extracts on Letrozole-Induced Polycystic Ovarian Syndrome and its Complications in Murine Model, Clinical Medicine Insights: Endocrinology and Diabetes. 2023; 16: 11795514231203864.
23. Jana S, Ghosh A, Dey A, Perveen H, Maity PP, Maji S, Chattopadhyay S. n-Butanol fraction of moringa seed attenuates arsenic intoxication by regulating the uterine inflammatory and apoptotic pathways. Environ Sci Pollut Res. 2024;13:1–21.
24. Gupta N, Gupta DK, Sharma PK. Condition factor and organosomatic indices of parasitized *Rattus rattus* as indicators of host health. J Parasit Dis. 2017;41(1):21–8.

25. Simental-Mendía LE, Rodríguez-Morán M, Guerrero-Romero F. The product of fasting glucose and triglycerides as surrogate for identifying insulin resistance in apparently healthy subjects. Metab Syndr Relat Disord. 2008;6:299–304.
26. Weydert CJ, Cullen JJ. Measurement of superoxide dismutase, catalase and glutathione peroxidase in cultured cells and tissue. Nat Protoc. 2010;5(1):51–66.
27. Kiddy DS, Sharp PS, White DM, Scanlon MF, Mason HD, Bray CS, Polson DW, Reed MJ, Franks S. Differences in clinical and endocrine features between obese and non-obese subjects with polycystic ovary syndrome: an analysis of 263 consecutive cases. Clin Endocrinol. 1990;32(2):213–20.
28. Crowe AR, Yue W. Semi-quantitative determination of protein expression using immunohistochemistry staining and analysis: an integrated protocol. Bio-protocol. 2019;9(24):e3465–3465.
29. Haslan MA, Samsulrizal N, Hashim N, Zin NSNM, Shirazi FH, Goh YM. Ficus deltoidea ameliorates biochemical, hormonal, and histomorphometric changes in letrozole-induced polycystic ovarian syndrome rats. BMC Complement Med Ther. 2021;21:1–13.
30. Kar TK, Sil S, Ghosh A, Barman A, Chattopadhyay S. Mitigation of letrozole induced polycystic ovarian syndrome associated inflammatory response and endocrinal dysfunction by Vitex negundo seeds. J Ovarian Res. 2024;17(1):76.
31. Mikhael S, Punjala-Patel A, Gavrilova-Jordan L. Hypothalamic-pituitary-ovarian axis disorders impacting female fertility. Biomedicines. 2019;7(1):5.
32. Hu K, Sun W, Li Y, Zhang B, Zhang M, Guo C, Chang H, Wang X. Study on the Mechanism of Sarsasapogenin in Treating Precocious Puberty by Regulating the HPG Axis. Evid. Based Complement. Alternat. Med. 2020; 2020: 1978043.
33. Peng F, Hu Y, Peng S, Zeng N, Shi L. Apigenin exerts protective effect and restores ovarian function in dehydroepiandrosterone induced polycystic ovary syndrome rats: a biochemical and histological analysis. Ann Med. 2022;54(1):578–87.
34. Rajan RK, Balaji B. Soy isoflavones exert beneficial effects on letrozole-induced rat polycystic ovary syndrome (PCOS) model through anti-androgenic mechanism. Pharm Biol. 2017;55(1):242–51.
35. Jahan S, Abid A, Khalid S, Afsar T, Shaheen G, Almajwal A, Razak S. Therapeutic potentials of Quercetin in management of polycystic ovarian syndrome using Letrozole induced rat model: a histological and a biochemical study. J. Ovarian Res., Kaplán P, Tatarková Z, Lichardusová L, Dušenka R, Jurečeková J. Androgen receptor and soy isoflavones in prostate cancer. Mol. Clin. Oncol. 2019; 10(2): 191–204.
36. Sil S, Ghosh A, Kar TK, Halder SK, Chattopadhyay S. Saccharomyces boulardii a novel yeast probiotic ameliorates metabolic syndrome associated with PCOS: A preliminary study. IJPAS. 2023;75(03):14–9.
37. Ding H, Zhang J, Zhang F, Zhang S, Chen X, Liang W, Xie Q. Resistance to the Insulin and Elevated Level of Androgen: A Major Cause of Polycystic Ovary Syndrome. Front Endocrinol (Lausanne).

2021;12:741764.

38. Kojta I, Chacińska M, Błachnio-Zabielska A, Obesity. Bioactive Lipids, and Adipose Tissue Inflammation in Insulin Resistance. Nutrients. 2020;12(5):1305.
39. Dhanya R, Arya AD, Nisha P, Jayamurthy P. Quercetin, a Lead Compound against Type 2 Diabetes Ameliorates Glucose Uptake via AMPK Pathway in Skeletal Muscle Cell Line. Front Pharmacol. 2017;8:336.
40. Jeong SM, Kang MJ, Choi HN, Kim JH, Kim JI. Quercetin ameliorates hyperglycemia and dyslipidemia and improves antioxidant status in type 2 diabetic db/db mice. Nutr Res Pract. 2012;6(3):201–7.
41. Lomenick B, Shi H, Huang J, Chen C. Identification and characterization of β-sitosterol target proteins. Bioorg Med Chem Lett. 2015;25(21):4976–9.
42. Zhou X, Sun C, Jiang L, Wang H. Effect of conjugated linoleic acid on PPAR gamma gene expression and serum leptin in obese rat. Wei Sheng Yan Jiu. 2004;33(3):307–9.
43. Yang L, Chen Y, Liu Y, Xing Y, Miao C, Zhao Y, Chang X, Zhang Q. The Role of Oxidative Stress and Natural Antioxidants in Ovarian Aging. Front Pharmacol. 2021;11:617843.
44. Mancini A, Bruno C, Vergani E, d'Abate C, Giacchi E, Silvestrini A. Oxidative Stress and Low-Grade Inflammation in Polycystic Ovary Syndrome: Controversies and New Insights. Int J Mol Sci. 2021;22(4):1667.
45. Darabi P, Khazali H, Mehrabani Natanzi M. Therapeutic potentials of the natural plant flavonoid apigenin in polycystic ovary syndrome in rat model: via modulation of pro-inflammatory cytokines and antioxidant activity. J. Gynaecol. Endocrinol., Cui YY, Zheng SC, Ma TN, Xie HJ, Jiang ZF, Li HW, Zhu YF, Huang KX, Li CG, Li J. JY. Sarsasapogenin improves adipose tissue inflammation and ameliorates insulin resistance in high-fat diet-fed C57BL/6J mice, Acta. Pharmacol. Sin. 2021; 42(2): 272–281.
46. Mustafa NH, Sekar M, Fuloria S, Begum MY, Gan SH, Rani NNIM, Ravi S, Chidambaram K, Subramaniyan V, Sathasivam KV, Jeyabalan S, Uthirapathy S, Ponnusankar S, Lum PT, Bhalla V, Fuloria NK. Chemistry, Biosynthesis and Pharmacology of Sarsasapogenin: A Potential Natural Steroid Molecule for New Drug Design, Development and Therapy. Molecules. 2022; 27(6): 2032.
47. Adeyi OE, Somade OT, Ajayi BO, James AS, Adeboye TR, Olufemi DA, Oyinlola EV, Sanyaolu ET, Mufutau IO. The anti-inflammatory effect of ferulic acid is via the modulation of NFκB-TNF-α-IL-6 and STAT1-PIAS1 signaling pathways in 2-methoxyethanol-induced testicular inflammation in rats. Phytomedicine Plus. 2023;3(3):100464.
48. Ko EB, Jang YG, Kim CW, Go RE, Lee HK, Choi KC. Gallic Acid Hindered Lung Cancer Progression by Inducing Cell Cycle Arrest and Apoptosis in A549 Lung Cancer Cells via PI3K/Akt Pathway. Biomol Ther (Seoul). 2022;30(2):151–61.
49. Qi G, Chen J, Shi C, Wang Y, Mi S, Shao W, Yu X, Ma Y, Ling J, Huang J. Cinnamic Acid (CINN) Induces Apoptosis and Proliferation in Human Nasopharyngeal Carcinoma Cells. Cell Physiol Biochem. 2016;40(3–4):589–96.

50. Eisermann K, Fraizer G. The Androgen Receptor and VEGF: Mechanisms of Androgen-Regulated Angiogenesis in Prostate Cancer. Cancers (Basel). 2017;9(4):32.
51. He Z, Chen AY, Rojanasakul Y, Rankin GO, Chen YC. Gallic acid, a phenolic compound, exerts anti-angiogenic effects via the PTEN/AKT/HIF-1α/VEGF signaling pathway in ovarian cancer cells. Oncol Rep. 2016;35(1):291–7.
52. Karl KR, Jimenez-Krassel F, Gibbings E, Ireland JL, Clark ZL, Tempelman RJ, Latham KE, Ireland JJ. Negative impact of high doses of follicle-stimulating hormone during superovulation on the ovulatory follicle function in small ovarian reserve dairy heifers. Biol Reprod. 2021;104(3):695–705.
53. Duncan WC. The inadequate corpus luteum. Reprod Fertil. 2021;2(1):C1–7.
54. Bergsten TM, Li K, Lantvit DD, Murphy BT, Burdette JE. Kaempferol, a Phytoprogestin, Induces a Subset of Progesterone-Regulated Genes in the Uterus. Nutrients. 2023;15(6):1407.
55. Yu Y, Cao Y, Huang W, Liu Y, Lu Y, Zhao J. β-Sitosterol Ameliorates Endometrium Receptivity in PCOS-Like Mice: The Mediation of Gut Microbiota. Front Nutr. 2021;8:667130.

Figures

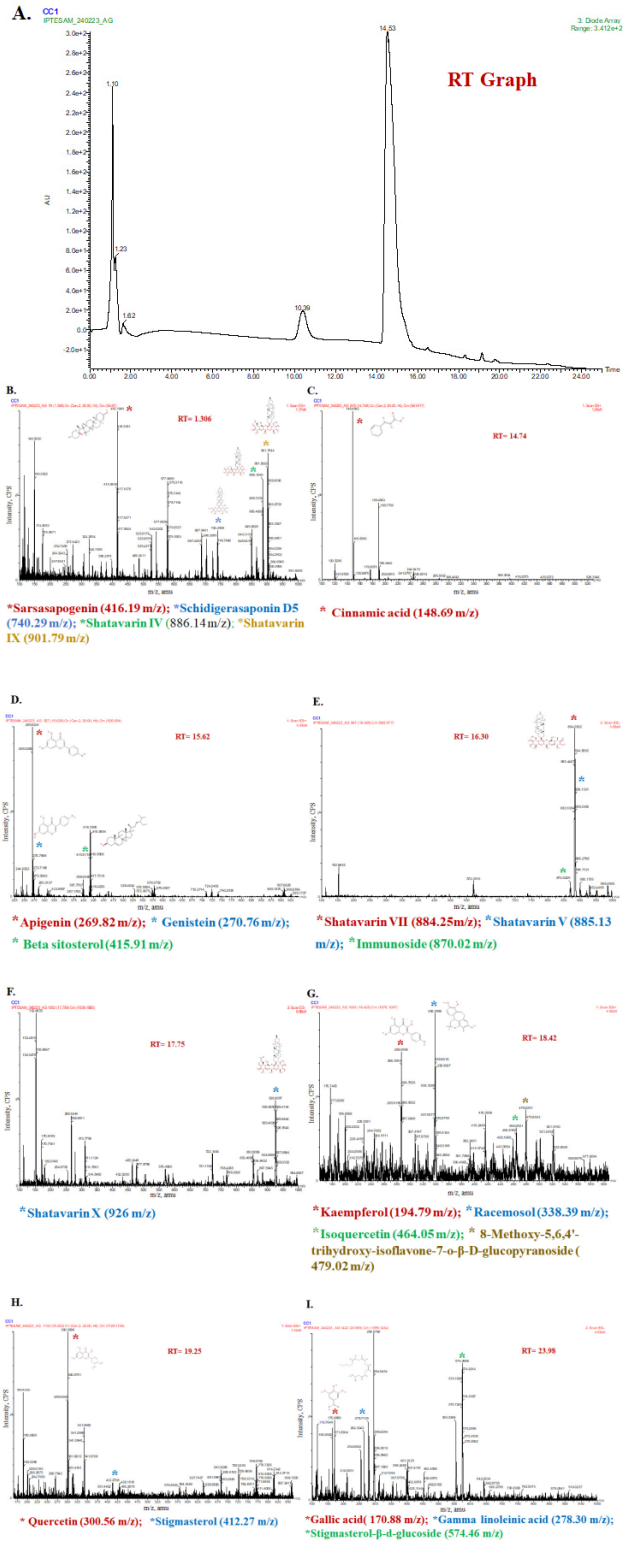

Figure 1

The graphical representation of LC-ESI/MS result of *Asparagus racemosus* ethanolic extract. This figure showed the main retention time (RT) graph with presence of bioactive components based on their molecular weight (m/z).

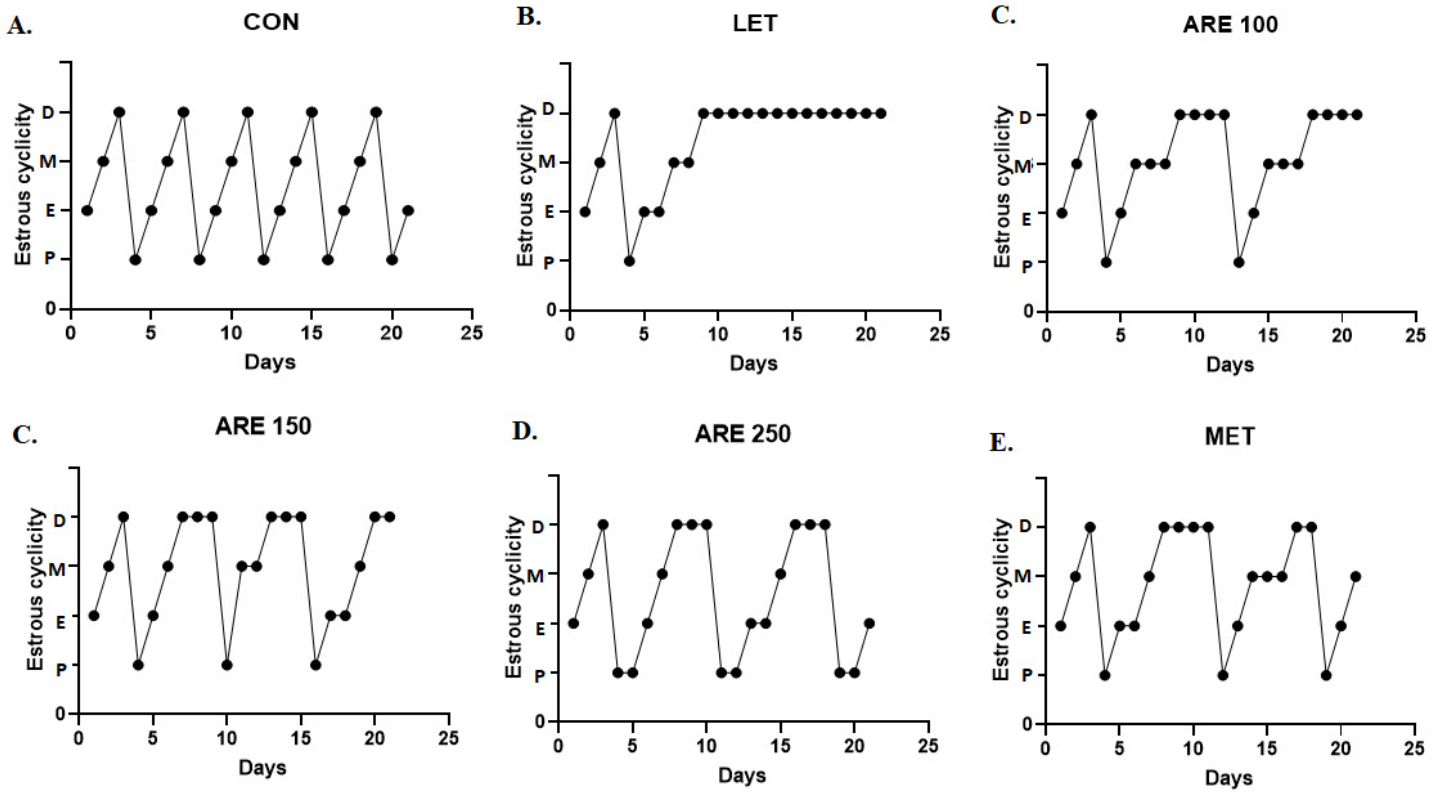

Figure 2

The line diagram represents the changes in estrous cycle in different groups throughout the investigation.

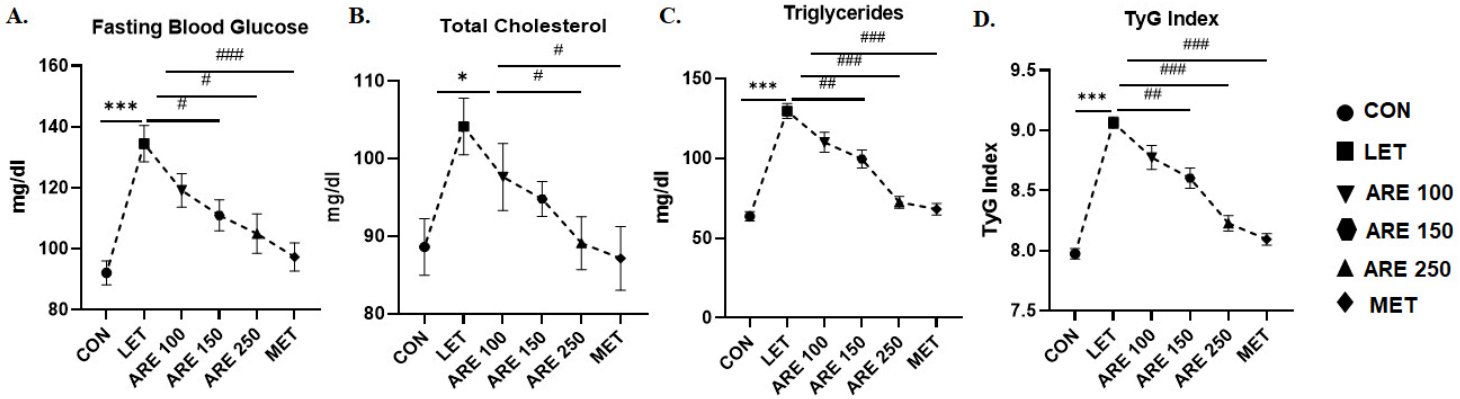

Figure 3

Effects of *Asparagus racemosus* on serum lipid profile of LET-treated PCOS group. (A) Fasting Blood glucose (B) Total cholesterol (C) Triglyceride and (D) TyG index. Data represent as Mean ± SEM (n = 6), estimated by ANOVA following the post hoc Tukey's test *P<0.05, **P<0.01, ***P<0.001 in respect to control; #P<0.05, ##P<0.01, ###P<0.001 in respect to PCOS group.

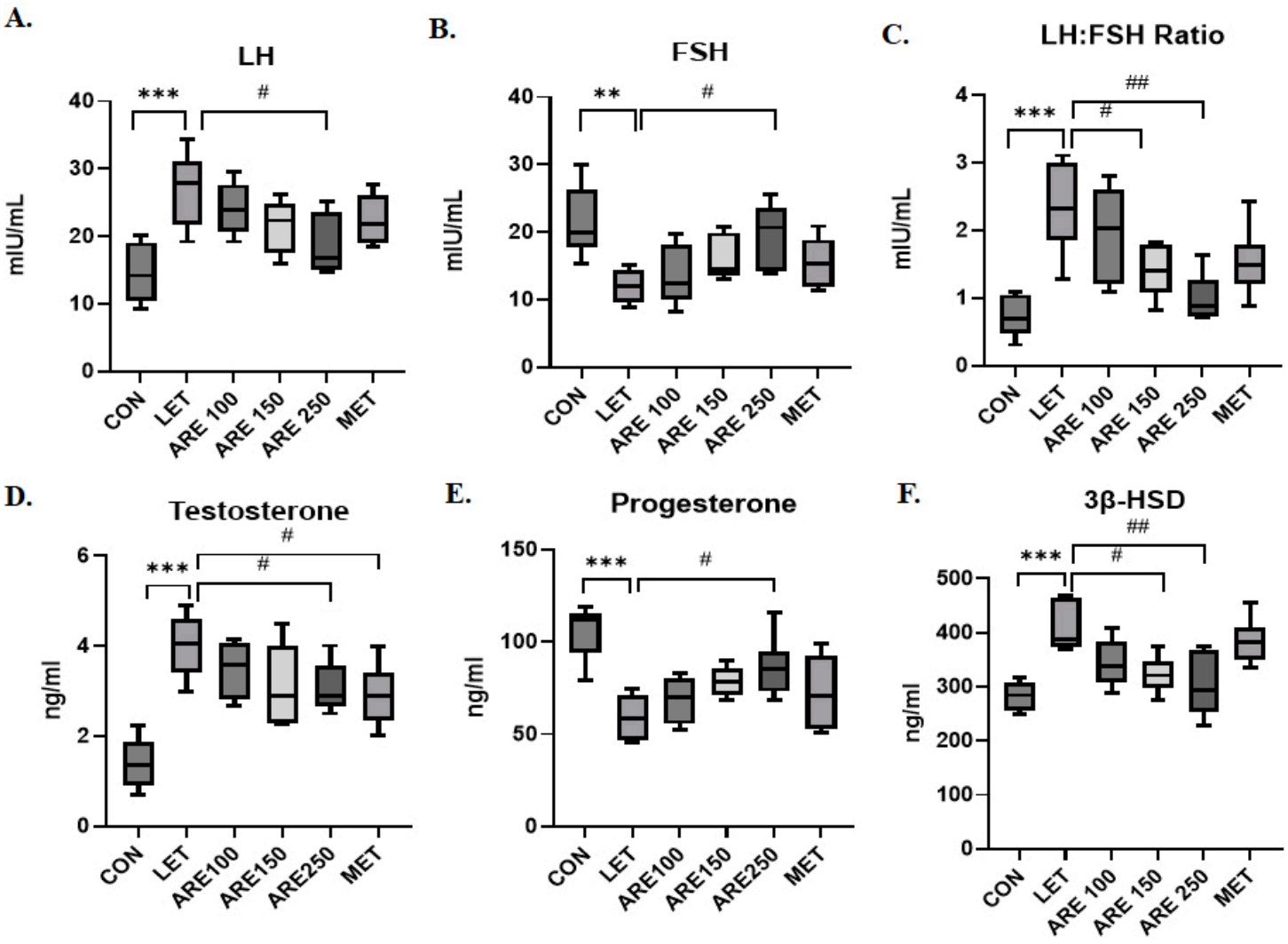

Figure 4

Effects of *Asparagus racemosus* on serum hormone profile and ovarian tissue specific steroidogenic enzyme (3βHSD). (A) LH (B) FSH (C) LH:FSH (D)Testosterone (E) Progesterone and (F) 3βHSD. This box and whisker diagram represent the minimum to maximum value (n=6), estimated by ANOVA following the post hoc Tukey's test *P<0.05, **P<0.01, ***P<0.001 in respect to control; #P<0.05, ##P<0.01, ###P<0.001 in respect to PCOS group.

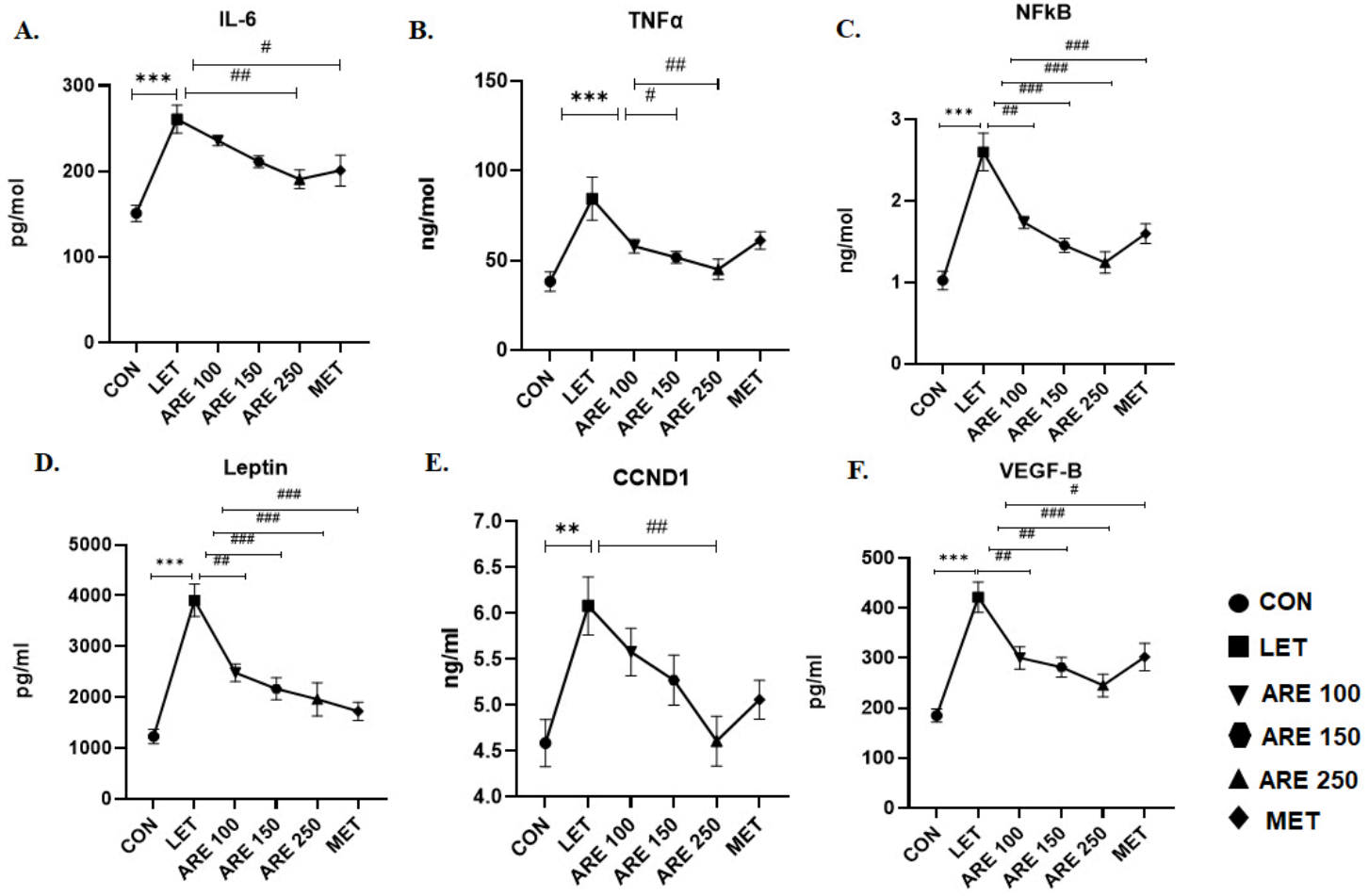

Figure 5

Effects of *Asparagus racemosus* on inflammatory, adipokine, angiogenic and cell cycle markers. (A) IL-6 (B) TNFα (C) NFkB (D)Leptin (E) CCND1 and (F) VEGF-B. Data represent as Mean ± SEM (n = 6), estimated by ANOVA following the post hoc Tukey's test *P<0.05, **P<0.01, ***P<0.001 in respect to control; #P<0.05, ##P<0.01, ###P<0.001 in respect to PCOS group.

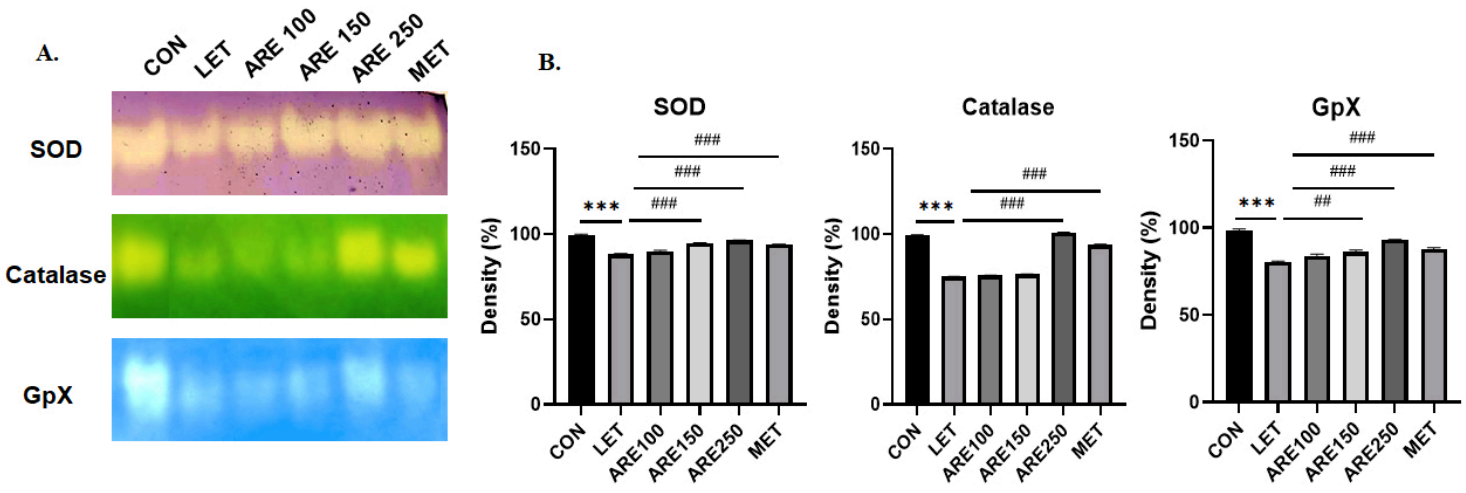

Figure 6

(A)The effect of *Asparagus racemosus* on the expression of ovarian antioxidant enzymes (SOD, Catalase and GPx) on native page. (B)The band density (%) of the expression pattern were graphically presented for these enzymes. Data represent as the Mean ± SEM (n = 6), estimated by ANOVA following the post hoc Tukey's test. *P<0.05, **P<0.01, ***P<0.001 with respect to control; #P<0.05, ##P<0.01, ###P<0.001 with respect to PCOS group.

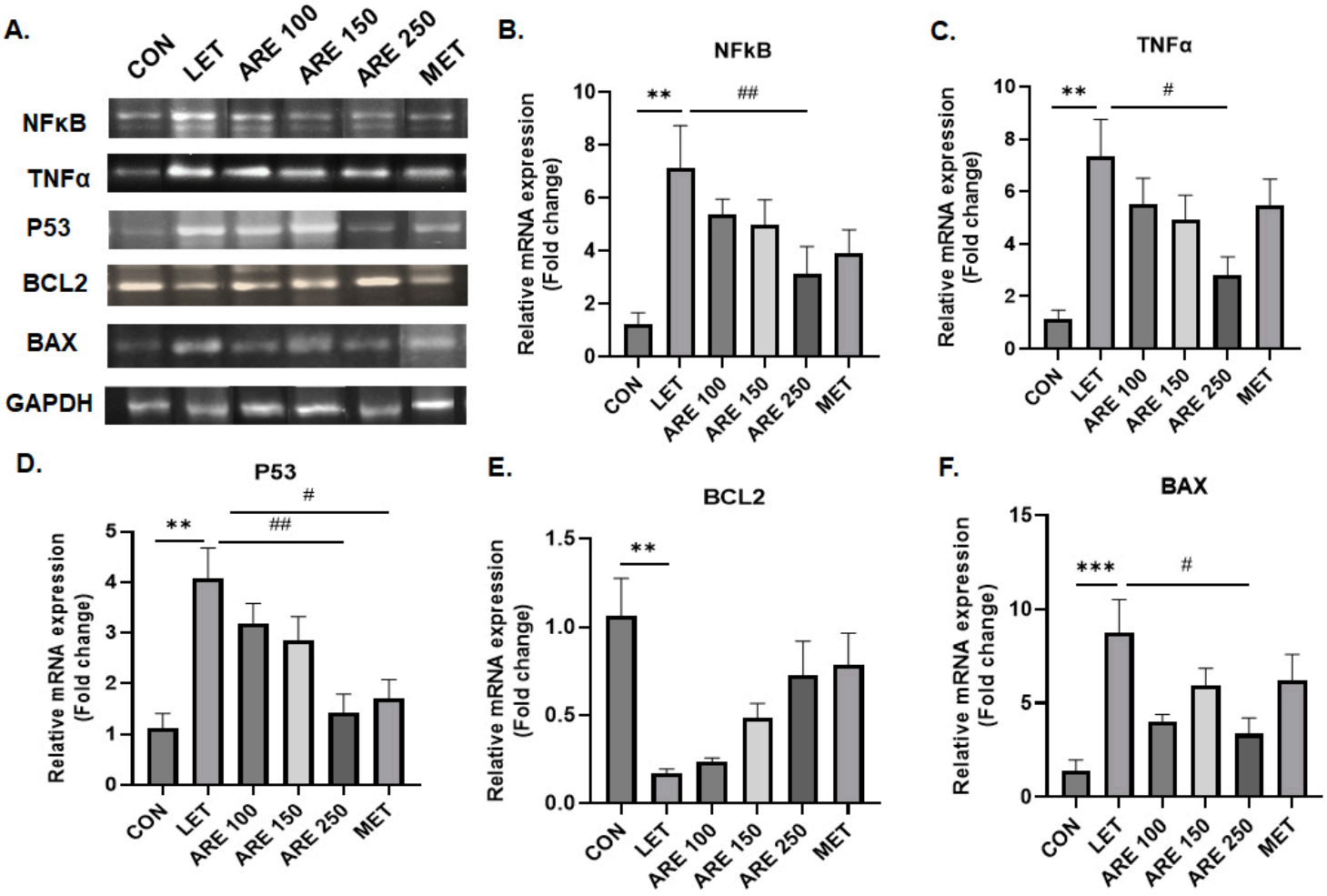

Figure 7

(A)The effect of *Asparagus racemosus* on the mRNA expression pattern of pro-inflammatory cytokines and apoptotic markers. The expressional fold change for (B) NFkB (C) TNFα (D) P53 (E) BCL2 and (F) BAX values are graphically presented based on Ct value. Here, GAPDH is served as the reference gene. Data represent as Mean ± SEM (n = 3); estimated by ANOVA following the post hoc Tukey's test. *P<0.05, **P<0.01, ***P<0.001 with respect to control; #P<0.05, ##P<0.01, ###P<0.001 with respect to LET group.

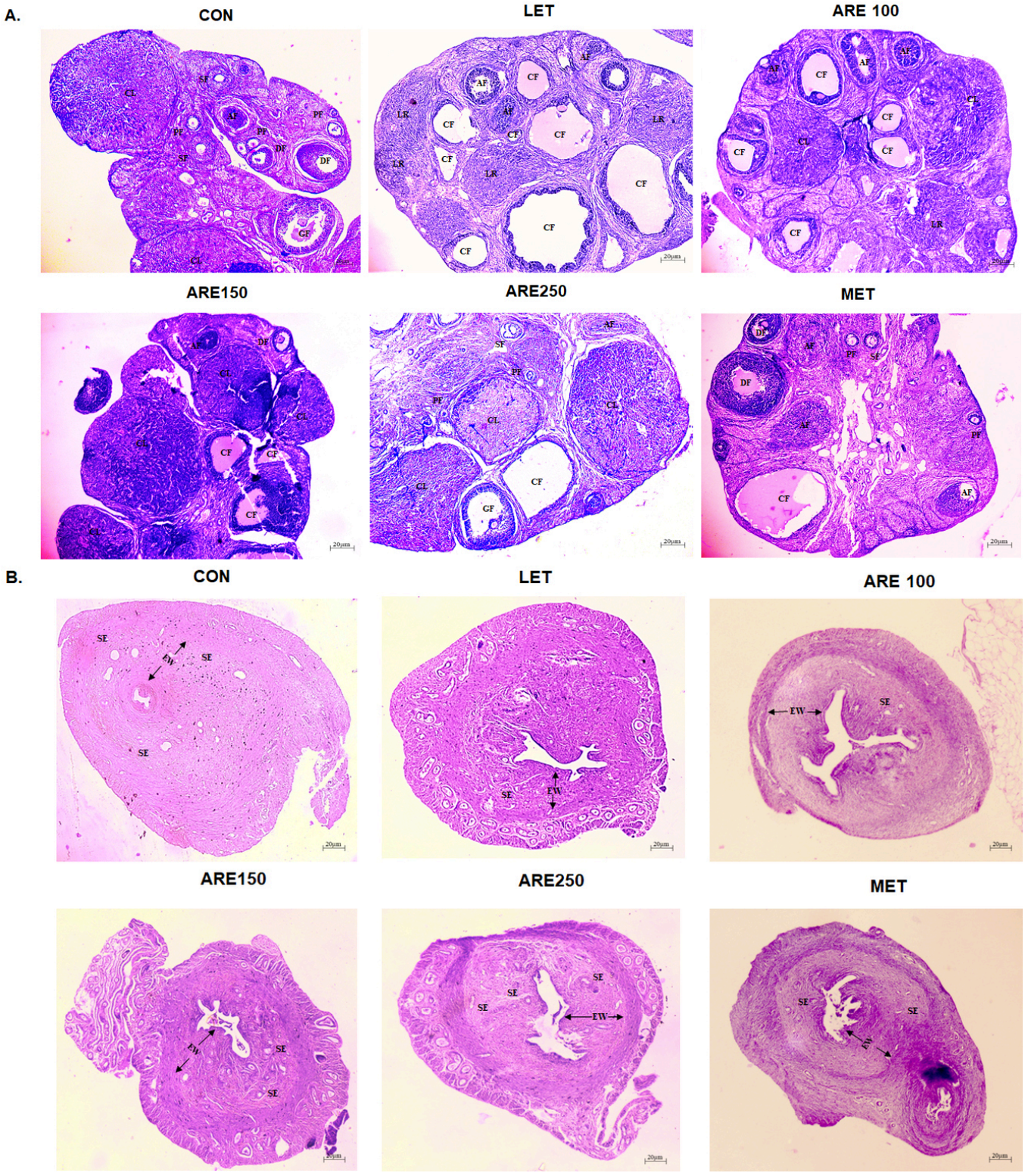

Figure 8

The photomicrographs represent the alteration of ovarian (A) and uterine (B) morphology at 40X magnificationin different groups. Primary follicle (PF), secondary follicle (SF), developing Follicle (DF), graafian follicle (GF), atretic follicle (AF), cystic follicles (CF), corpus luteum (CL) and luteal regression (LR) are indicated in the histological images.

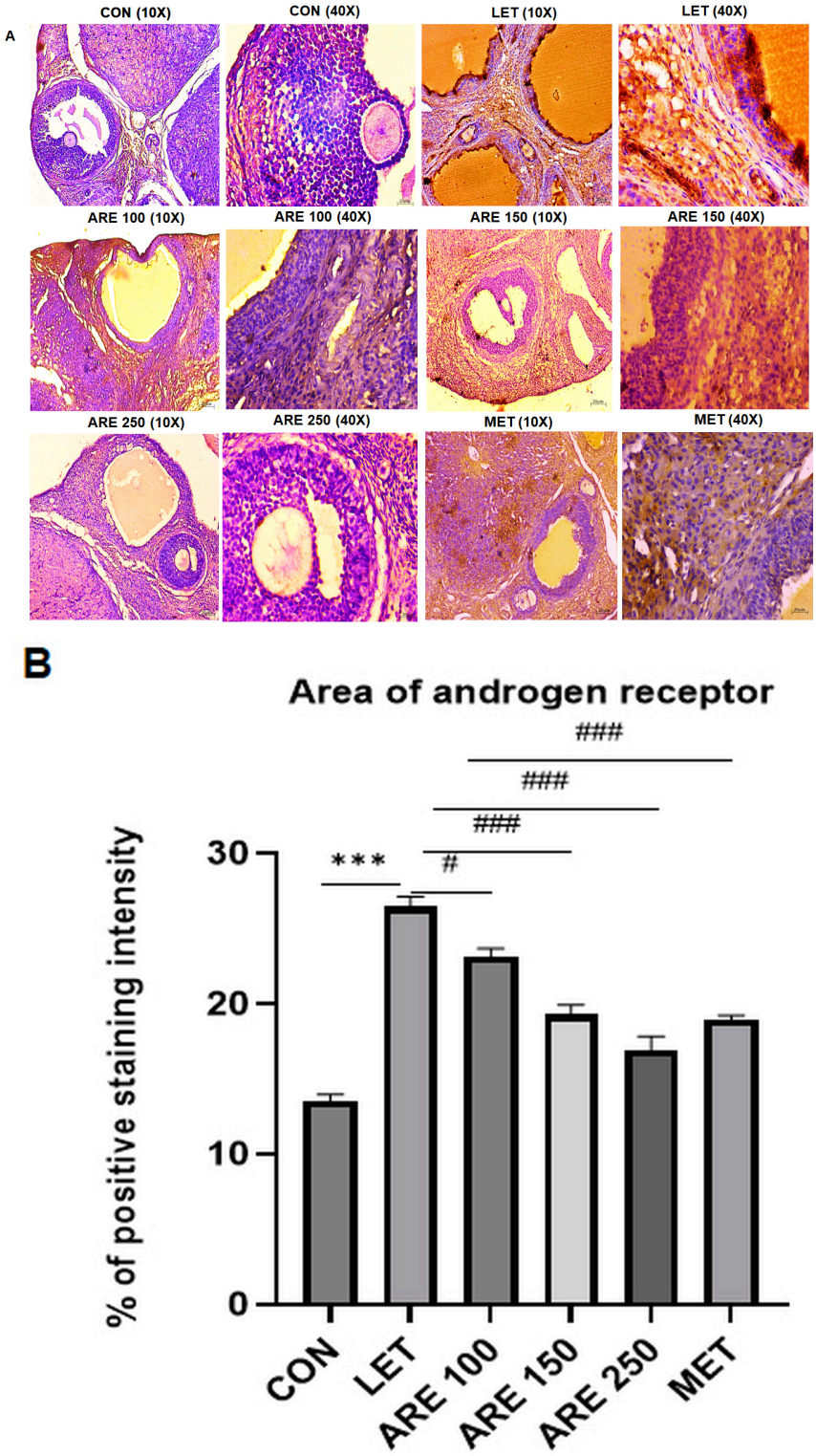

Figure 9

The photomicrographs represent effect of *Asparagus racemosus* on the immunoexpression of AR or NR3C4 in the ovarian tissues at 100x and 400x magnification (A). Reddish-brown color staining cells indicates the positive AR expression. (B) The quantification of the immunostained images represented by analysing the positive DAB-stained area (%). Data represent as Mean ± SEM (n = 3); estimated by

ANOVA following the post hoc Tukey's test. *P<0.05, **P<0.01, ***P<0.001 with respect to control; #P<0.05, ##P<0.01, ###P<0.001 with respect to LET group.

Supplementary Files

This is a list of supplementary files associated with this preprint. Click to download.

- Supplementaryfile16.06.24.docx